Unifying the Temperature Dependent Dynamics of Glass Formers

Joseph B. Schlenoff^{*1} and Khalil Akkaoui¹
¹Department of Chemistry and Biochemistry, The Florida State University, Tallahassee, Florida 32306-4390, United States

Email: jschlenoff@fsu.edu

Keywords: glass transition, supercooled liquids, Arrhenius, dynamic heterogeneity, polymer electrolyte, ferroelectric relaxor

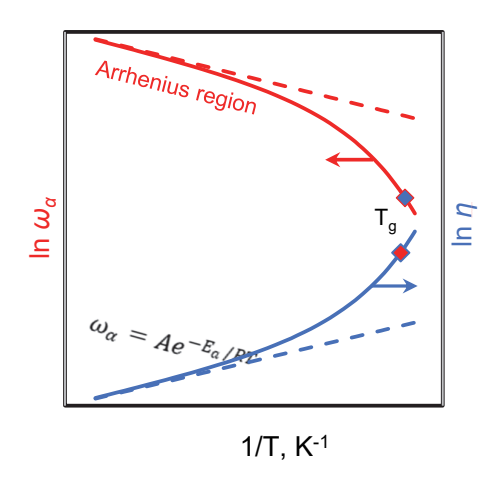
Abstract

Strong changes in bulk properties, such as modulus and viscosity, are observed near the glass transition temperature, T_q, of amorphous materials. For more than a century, intense efforts have been made to define a microscopic origin for these macroscopic changes in properties. Using transition state theory, TST, we delve into the atomic/molecular level picture of how microscopic localized relaxations, or "cage rattles," translate to macroscopic structural relaxations above T_g. Unit motion is broken down into two populations: (1) simultaneous rearrangement occurs among a critical number of units, n_α, which ranges from 1 to 4, allowing a systematic classification of glass formers, GFs, that is compared to fragility; (2) near T_a, adjacent units provide additional free volume for rearrangement, not simultaneously, but within the "primitive" lifetime, τ_1 , of one unit rattling in its cage. Relaxation maps illustrate how Johari-Goldstein β-relaxations stem from the rattle of n_α units. We analyzed a wide variety of glassy materials, and materials with glassy response, using literature data. Our four-parameter equation fits "strong" and "weak" GFs over the entire range of temperatures and also extends to other glassy systems, such as ion-transporting polymers and ferroelectric relaxors. The role of activation entropy in boosting preexponential factors to high "unphysical" apparent frequencies is discussed. Enthalpy-entropy compensation is clearly illustrated using the TST approach.

Introduction

Below their glass transition temperature, T_g , amorphous materials exist in a glassy state without long range order. A molecular scale description of the approach to this state from high temperatures, signaled by a rapid increase in bulk stiffness, has long challenged theorists. Figure 1 illustrates the dilemma: at sufficiently high temperature, T_g , the bulk structural relaxation rate, ω_α , mirrored by the viscosity, η , shows classical Arrhenius behavior $In\omega_\alpha \sim -1/T_g$, typically used to describe thermally activated processes. Approaching T_g , in the supercooled region there is a strong deviation from Arrhenius, and at T_g the material becomes a solid glass with almost no liquid-like response. It is generally agreed that cooperative motion between units comprising the glass former, GF, increasingly limit dynamics approaching T_g .

Figure 1. Relaxations in glass formers. The dynamics, given by the structural relaxation rate ω_{α} (s⁻¹), or viscosity η (Pa s), slow as it cools. At high temperatures, dynamics can be



described by an Arrhenius equation (dashed lines). Deviation from Arrhenius behavior is observed approaching T_q (diamond).

A major goal of theory is to describe dynamics in all glass formers with one equation.¹ Towards this goal, "universal" scalings and relationships have been established. For example, the α -relaxation of many glass formers adheres to thermodynamic scaling: ω_{α} is a function of a scaled relationship between density (pressure) and temperature. While activation energy E_a and a prefactor A are the only two fit parameters required to describe Arrhenius response, the most economical analytical description of the curvature in the supercooled region needs at least three parameters. Towards this end, the Vogel-Fulcher-Tammann (VFT) equation has been used for several decades;9

$$\omega_{T,VFT} = \omega_{0,VFT} e^{\frac{-DT_o}{T-T_o}}$$
 [1]

 $\omega_{T,VFT} = \omega_{0,VFT} \, e^{\frac{-DT_o}{T-T_o}} \eqno(1)$ where $\omega_{0,VFT}$, D, and T_o are empirical, freely-adjustable fit parameters. ω_0 (η₀) comes from a high-temperature extrapolation. To, known as the Vogel temperature, is usually about 50 K below T_q. Many decades of discussion and controversy have ensued over the meaning of T₀ and whether, as it implies, flow ceases completely at this temperature. 10 VFT fits with one set of parameters are typically useful over a limited temperature range. If the range is expanded, two or more VFT fits,11-13 or a combination of Arrhenius plus VFT,14 are often used. Many of the models describing the temperature dependence of structural relaxation have recently been summarized by Novikov and Sokolov. 15

Eyring modified his transition state theory (TST) to describe the viscosity of liquids¹⁶

$$\eta = \kappa \eta_0 e^{-\Delta S^*/R} e^{\Delta H^*/RT}$$
 [2]

where free energy of activation $\Delta G_a^* = \Delta H^* - T\Delta S_a^*$, and ΔH^* and ΔS^* are enthalpy and entropy of activation, respectively. κ is a transmission coefficient which represent a probability of reaction. Eyring assumed¹⁶ that κ was "probably very nearly unity." Prefactor η₀ was estimated to be N_Ah/V where N_A is Avogadro's number, V the molal volume and h is Planck's constant. In a transition state model, Avramov and Milchev, AM, assumed that dynamics resulted from hopping of units between coordination spheres with a random distribution of activation energies and relaxation time, τ , around a mean. ¹⁷ This introduced dynamic heterogeneity and yielded the following three-parameter expression

$$log\eta = log\eta_0 + \left[\frac{\tau}{T}\right]^{\alpha}$$
 [3]

Maxwell's equation relates relaxation rate to viscosity via the high frequency glassy modulus G_0 : $\omega_{\alpha} = G_0/\eta$. Extrapolations of AM to high temperatures (i.e. into the Arrhenius region) significantly overestimate η_0 , which should be of order 10^{-2} Pa s.¹⁰ Hrma et. al recently concluded18 that any analytical model representing a full 11-12 orders of dynamic range in viscosity or relaxation time, from T_g up, must have at least four adjustable parameters.

Macedo and Litovitz19 focused on the deviation from Arrhenius in the supercooled region by breaking down the jump probability of a molecule to an empty site, pi, into the probability of having sufficient energy to break bonds p_E (which is the $e^{-\frac{Ea}{RT}}$ term) and the probability that there is sufficient local free volume for a jump to occur, p_{ν}

$$p_i = p_E \times p_v \tag{4}$$

For the p_v term they employed the expression of Cohen and Turnbull²⁰ for the probability of finding the minimum local free volume for a jump

$$p_v = e^{-\gamma v_0/v_f} \tag{5}$$

Where y is an overlap correction between 0.5 and 1, v₀ is the close-packed molecular volume and v_f is the free volume. This yields the following

$$\eta = \eta_0 e^{\gamma v_0 / v_f} e^{E_a / RT} \tag{6}$$

This "hybrid" 5-term equation was able to fit both the supercooled and Arrhenius region of the glasses tested.

An expression by Mauro et al. 21 , previously proposed empirically by Waterton, 22 was derived starting from the Adam-Gibbs (AG) equation relating the configurational entropy, S_c , of a glass former to the viscosity 23

$$ln\eta = ln\eta_0 + \frac{E_a s_c^*}{RTS_c}$$
 [7]

where s_c^* is a constant high temperature configurational entropy (found in the Arrhenius region) and S_c decreases into the supercooled region. Calculating^{24, 25} or measuring²⁶ S_c is not straightforward. Mauro et al. used a temperature-dependent constraint model to obtain S_c , assumed the glass transition was defined by a shear viscosity of 10^{12} Pa s, and used experimental slopes of $\log_{10} \eta$ vs. 1/T at T_g (known as fragilities²⁷) to arrive at an equation of the form

$$log_{10}\eta = log_{10}\eta_0 + \frac{K}{T}e^{C/T}$$
 [8]

Where K and C are constants. A comparison with VFT and AM models concluded that Eq. 8 provided a more accurate description.²¹ However, all the above three-parameter equations fail to some extent into the Arrhenius region.¹⁸

Adam and Gibbs²³ recognized the central importance of correlating molecular (microscopic) motion to structural (bulk) relaxation in glass formers when they ascribed the temperature dependent relaxation rates, $\omega_{\alpha,AG}$ to rearrangements in microstructures termed cooperatively rearranging regions (CRRs) of minimum size n_T units (which they called z^*)²³

$$\omega_{\alpha,AG} = Ae^{-n_T E_1/RT}$$
 [9]

where E_1 is the activation energy for one unit. At temperatures closer to the glass transition, the apparent activation energy n_TE_1 (see the slopes in Figure 2) increases substantially, becoming larger than the enthalpy of vaporization by almost a factor of $5.^{23,\,28}$ The increase in apparent E_a is interpreted to stem from increased cooperativity between units. 23

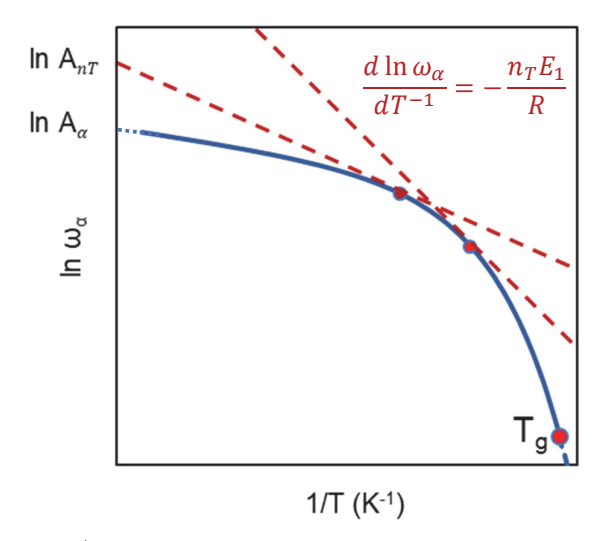


Figure 2. In ω_{α} (s⁻¹) as a function of 1/T; solid blue curve. Near the glass transition, n_T cooperatively rearranging units present an increasing *apparent* energy barrier of height $n_T E_1$ (dashed red lines), where E_1 is the activation energy for one unit. The prefactor $A_{n(T)}$ also increases strongly with n_T on these Arrhenius plots.

The configurational entropy-based approach in Equation 7 is appealing because the activation energy and $ln\eta_0$ terms remain constant, leaving the configurational entropy to be determined. In contrast, in the AG dynamic cooperativity framework (Equation 9) each of the

Arrhenius-style plots (Figure 2) has slope n_TE_1 but also a different A intercept which depends on n_T . These values of A can be enormous and are at odds with the original AG approach, which relied on a constant preexponential factor.²³ Nevertheless, models based on the apparent increase in activation energy predict slowing of dynamics near T_g . ^{29,30} In our model E_a does not change, instead, an additional kinetic barrier develops approaching T_g .

In the present work, we re-evaluate the CRR aspects of the AG microscopic model (without progressing to the configurational entropy parts of AG) in a transition state theory framework and add a crucial refinement to the idea that local motion on the microscopic scale is described as caged motion, where units rattle locally to the limits of their cage, but not beyond.^{4, 31} Under the right conditions, units escape their cages and rearrange - a structural change impacting bulk properties (e.g. viscosity and modulus). In our analysis, we break cooperative motion down into two types: a small number of correlated units rearranges simultaneously, facilitated in the supercooled region by neighbors that move within the relaxation time of one unit cage rattle. Separating the microscopic components in this way allows us to separate the spatial and temporal elements of the α -relaxation and show how localized caged motion evolves into structural relaxation.

Methods and Model

Single Units. At the microscopic level we assume a material consists of single units of minimum size, often presented as beads in simulations.^{3, 31, 32} These units represent the smallest entities, atoms or groups of atoms, that can potentially rearrange to isoenergetic states before and after rearrangement. At all temperatures above zero, we assume units rattle to the extreme of their cages at an *average* (relaxation) rate ω_1

$$\omega_1 = A_1 e^{-E_1/RT} \tag{10}$$

with activation energy E_1 and preexponential factor A_1 . This frequency refers to units rattling to the limit of their transient cages⁴ with an *average* temperature dependent relaxation time $\tau_1 = 1/\omega_1$. In other words, a fraction of units, given by the Boltzmann distribution, $e^{-E_1/RT}$, has enough energy to move to the limit of their cage.

A Poisson distribution describes the probability that a given number of random events will occur in a fixed interval of time, and is given by a probability mass function, p(k), with k the number of occurrences: $p(k) = \frac{\lambda^k}{k!} e^{-\lambda}$. The probability, p(k = 1), of a specific unit (k = 1) moving

in its cage in τ_1 seconds, with an average rate $\lambda = 1$ move per τ_1 seconds, is $p(k) = \frac{1^1}{1!} \left(\frac{1}{e}\right)$. Therefore, the probability that n(T) specific neighboring units will move in interval τ_1 is $e^{-n(T)}$.

The Critical Relaxation Cluster, n_{α} . Dielectric, mechanical, and thermal methods reveal many relaxation modes in glasses. Johari and Goldstein drew attention to certain relaxations, $β_{JG}$, in rigid glasses which had similar Arrhenius temperature dependences as the liquid state (at far higher temperatures) and suggested this relaxation corresponded to less cooperative but caged motion of an unspecified number of adjacent or clustered units. ³³ Ngai and coworkers have stressed the importance of these "primitive relaxations" as precursors to the α-relaxation at T > T_g . ⁸ Recent computer simulations have supported the evolution of caged dynamics from far below T_g to unhindered dynamics in the liquid state far above T_a . ³⁶

Here, we assume for α -relaxation a cluster of a specific number of units, n_{α} , must rearrange simultaneously such that the total energy is the same before and after the move. These n_{α} units, in a local minimum energy environment, are connected by chemical (covalent, ionic, or metallic bonding) or physical (dipolar, hydrogen bonding) interactions, depending on the material, and move to conserve the symmetry and energy of interaction. This (temperature independent) critical number of units is often assumed to be equal to 1,²³ but, as shown here, it can range from 1 to 4. Above T_g , n_{α} units start to rearrange, below T_g , they mostly rattle (see Figure 3 for an example of $n_{\alpha}=2$). If n_{α} is the same for α and β_{JG} relaxations, the activation energy for n_{α} units rattling simultaneously is $n_{\alpha}E_1=E_a$, which yields the corresponding Arrhenius form of the caged relaxation rate $\omega_{n_{\alpha,rattle}}=\omega_{JG}=A_{JG}e^{-E_{\alpha}/RT}$, where A_{JG} is the prefactor for rattling.

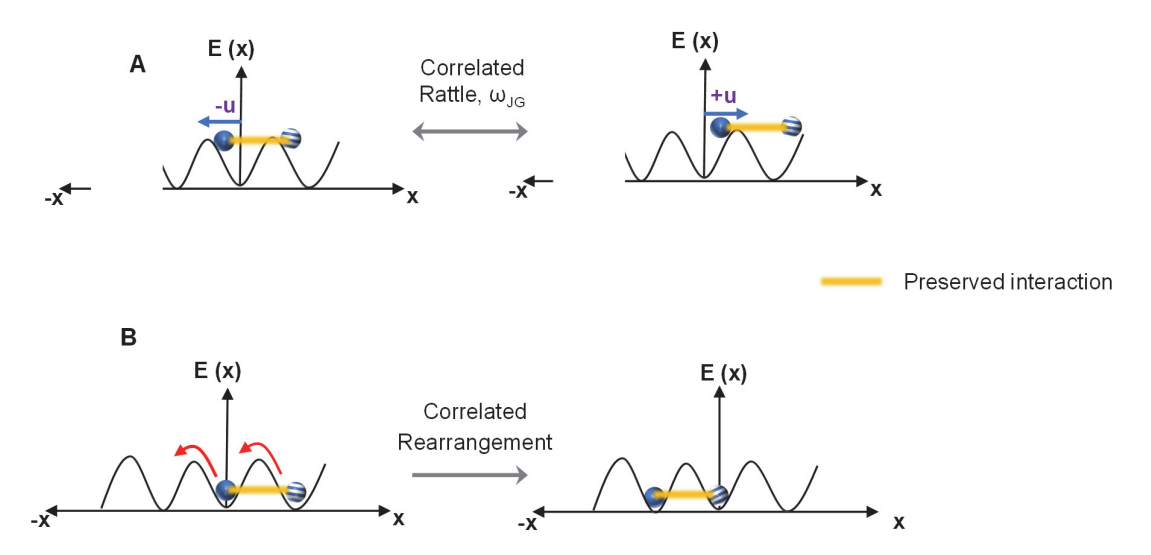


Figure 3. A. A rattle of two units, which move in a correlated manner to preserve the interaction between them. **B.** Some rattles evolve into a rearrangement, seen as a structural relaxation.

Cooperatively Assisting Units, n_c. When the amplitude of the rattle is enough to overcome the boundaries of the cage, a unit, or a cluster n_{α} of them, may escape. When does a caged relaxation evolve into a structural relaxation? Doolittle and others advanced the idea that the degree of structural mobility is connected directly to the free volume of the material^{37, 38} and cooperativity is a consequence of limited free volume. 7,39 Thus, n_{α} units require at least V_{α} of free volume to rearrange i.e. to go from caged to structural relaxation. At sufficiently high temperatures (the Arrhenius region) there are no (free volume) constraints to the concerted movement of n_{α} units. α -relaxation occurs with the same slope as caged n_{α} but the intercept is higher because $A_{\alpha} > A_{JG}$. As the temperature decreases, free volume also decreases. At some specific temperature, T_{SA} (SA = super-Arrhenius), at least one of the neighboring units must move to create sufficient free volume during interval τ_1 , which occurs with probability 1/e. This additional unit, and other neighbors that are increasingly called upon as the temperature decreases, are termed "cooperatively assisting," n_{c(T)}. Their purpose is to focus the local free volume, which fluctuates spatially and temporally throughout the sample, around n_α. Thus, the minimum total number of neighboring units moving cooperatively within τ_1 at any temperature, $n_T = n_\alpha + n_{c(T)}$

6

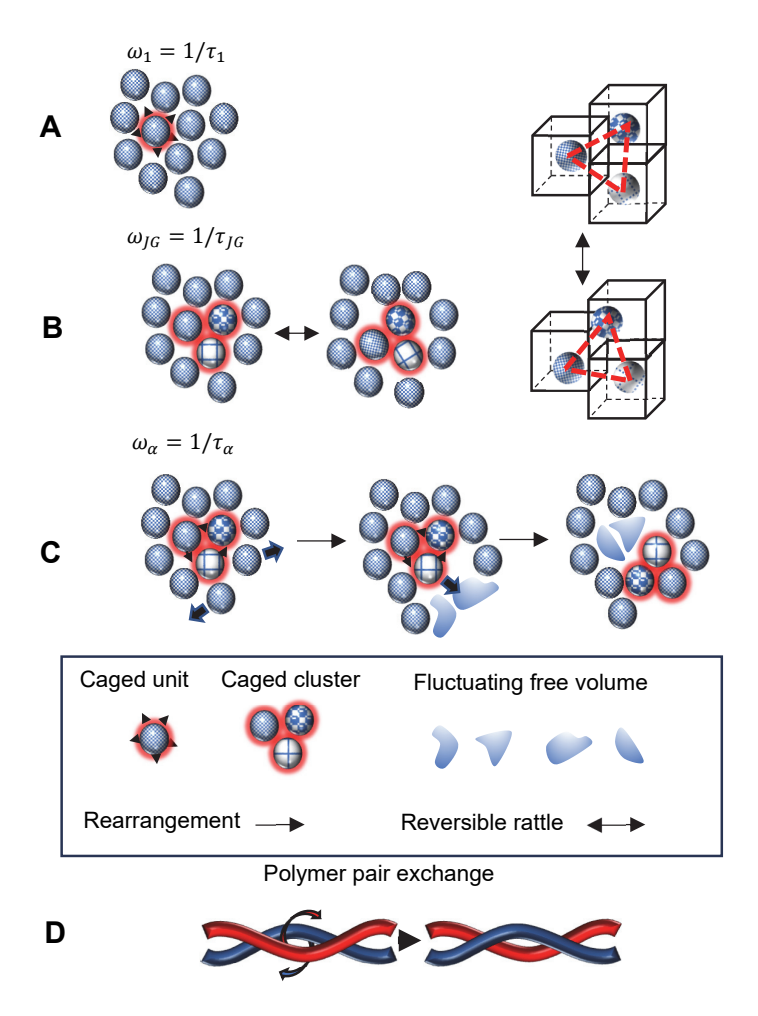


Figure 4. Relaxation modes. **A & B** caged motion of 1 or 3 units, the latter sampling the extremes of the cage while maintaining its n_{α} = 3 interaction environment; **C**) τ_{α} : structural relaxation of n_{α} = 3 units facilitated by two neighbors ($n_{c(T)}$ = 2) which provide enough free volume for n_{α} units to structurally rearrange. **D**. Possible unit exchange in polymers.

 T_{SA} marks the start of deviation from Arrhenius response of the α -relaxation where it now enters the spatio-temporally restricted regime. Microstructures of n_{α} units moving while conserving the symmetry of interaction are suggested in Figure 4A - C. From the results below, simple molecular GFs with mainly van der Waals intermolecular interactions (no hydrogen bonding) appear to yield n_{α} = 1. Polymers appear to be a special case wherein n_{α} is usually = 2. For obvious reasons, movement in linear polymers is dimensionally constrained due to the connectivity of the repeat units: only a small segment of the chain, such as a persistence length, can move as a unit. Figure 4D shows the exchange of two polymer segments as a possible example of a n_{α} = 2 concerted move. Because the Si atom in silicates shares oxygens with four other Si, the n_{α} = 4 found for silicates and related glasses could mean that a unit is an oxygen atom. Using high-temperature ²⁹Si NMR measurements of $K_2Si_4O_9$, relaxation consistent with exchange of oxygens was identified with a total activation energy E_a of 180 kJ mol⁻¹, ⁴⁰ in the range of E_a for silicates listed below.

There are no preordained n_{α} clusters. Within any τ_1 , any cluster of n_{α} units may attempt to rearrange. Below T_{SA} they are not assured of the free volume needed to rearrange, so they have to rely on $n_{c(T)}$ neighbors to move during τ_1 to provide the required free volume.

Heterogenous Dynamics. Another generally accepted feature of supercooled liquids is that they exhibit spatially heterogenous dynamics, 1-3 or regions of different sizes moving at different rates.41 In the present analysis, we incorporate the central idea of dynamic heterogeneity as follows: first, there is a spatially- and temporally- fluctuating distribution of sizes in the CRR. Second, as with AG, at any temperature all CRRs above a minimum size, n_T (= n_α + $n_{c(T)}$), contribute to bulk α-relaxation:

$$\omega_{\alpha} = A_{\alpha}' e^{-E_{\alpha}/RT} \sum_{n=n_{c(T)}}^{\infty} e^{-n_{T}}$$
 [11]

Any CRR of size n_T and above contributes to α -relaxation with weight $e^{-n_{c(T)}}$. The summation is a geometric sum and therefore Equation 11 becomes

$$\omega_{\alpha} = A'_{\alpha} e^{-E_{\alpha}/RT} \frac{e^{1-n_{c(T)}}}{e^{-1}} = A_{\alpha} e^{-E_{\alpha}/RT} e^{-n_{c(T)}}$$
[12]

where $A_{\alpha} = \frac{e}{e-1} A'_{\alpha}$.

In TST, E_a is replaced by an activation free energy ΔG^* with entropic and enthalpic contributions to the activation barrier. $E_a = \Delta H_a^* = \Delta H_{n_\alpha}^*$ at constant pressure. For the unit (n = 1) rattle

$$\omega_1 = A_0 e^{\Delta S_1^*/R} e^{-\Delta H_1^*/RT}$$
 [13]

and for the n_α rattle

$$\omega_{IG} = A_0 e^{\Delta S_{IG}^*/R} e^{-\Delta H_{n\alpha}^*/RT}$$
 [14]

This presentation makes it clear that the intercept of an Arrhenius plot includes a physical attempt frequency, A₀, which is assumed to be near the Boson frequency, and an activation entropy contribution. Only when ΔS* is negligible does the A intercept represent an attempt frequency. The (overlooked) importance of ΔS^* has recently been emphasized by Xu et al.⁴²

The full TST equation for the structural relaxation is

$$\omega_{\alpha} = A_0 e^{\Delta S_{struct}^*/R} e^{-\Delta H_{n\alpha}^*/RT} e^{-n_{c(T)}}$$
 [15]

 $\omega_{\alpha} = A_0 e^{\Delta S_{struct}^*/R} e^{-\Delta H_{n_{\alpha}}^*/RT} e^{-n_{c(T)}} \qquad [15]$ where ΔS_{struct}^* is the structural activation entropy for n_{α} units and $\Delta H_{n_{\alpha}}^* = n_{\alpha} \Delta H_1^*$. The deviation of ω_{α} from Arrhenius at any temperature is simply a factor of $e^{-n_{c(T)}}$.

Equation 12 shows how relaxation depends on a Boltzmann distribution term, $e^{-E_a/RT}$, representing the steady-state fraction of n_α clusters with energy sufficient to overcome barrier E_a , and a statistical term, $e^{-n_{c(T)}}$, stemming from the limiting of free volume with decreasing temperature below T_{SA} (free volume continues to increase above T_{SA} but no longer limits the dynamics). A final assumption from Adam and Gibbs²³ allows for the substitution of $n_{c(T)}$: the slope of the ω_{α} curve at any T is (see Figure 2) $\frac{d \ln \omega_{\alpha}}{d \ T^{-1}} = -\frac{n_T E_1}{R}.$

$$\frac{d \ln \omega_{\alpha}}{d T^{-1}} = -\frac{n_T E_1}{R}.$$
 [16]

n_TE₁ only appears to be a growing activation barrier. It represents the slope of an Arrhenius equation (as in Figure 2) for n_T units rearranging *simultaneously*. In our treatment, only n_{α} units actually rearrange simultaneously. If n_TE₁ were the actual barrier, the probability of rearranging at most temperatures would vanishingly small approaching T_g . For example, if A_α were 10^{13} s⁻¹ 1 , E₁ = 20 kJ, T_g = 300 K, n_{Tg} = 13, then n_TE₁ would be 260 kJ and ω_{α} would be about 10⁻²¹ s⁻¹ ¹ instead of approximately 0.01 s⁻¹, as usually seen.

At temperatures greater than T_{SA} , the free volume around n_{α} is enough to allow concerted rearrangement without any contributions from $n_{c(T)}$ units $(n_T \to n_{c(T)} \to 0)$ and the frequency attains Arrhenius behavior

$$\omega_{\alpha,Arr} = A_{\alpha} e^{\frac{-E_{\alpha}}{RT}}$$
 [17]

 $\omega_{\alpha,Arr} = A_{\alpha}e^{\frac{-E_{\alpha}}{RT}} \qquad \qquad [17]$ A_{α} is extrapolated from higher temperature measurements where T > T_{SA} as shown in Figure 2 and Figure S1. To minimize the error in measured E_a and A_α the temperature should extend as far into the Arrhenius region as possible.

The deviation of the measured frequency from the Arrhenius frequency (i.e the frequency calculated at any temperature using Equation 12) is

$$\ln\left(\frac{\omega_{\alpha,Arr}}{\omega_{\alpha}}\right) = n_T - n_{\alpha} = n_{c(T)}$$
 [18]

The number of cooperative units at T_g , n_{Tg} is given by $n_{Tg} = \ln \frac{\omega_{\alpha,Arr}}{\omega_{\alpha,Tg}} + n_{\alpha}$

$$n_{Tg} = \ln \frac{\omega_{\alpha,Arr}}{\omega_{\alpha,T_g}} + n_{\alpha}$$
 [19]

The slope of the linear Arrhenius plot is

$$-\frac{dln\omega_{\alpha,Arr}}{dT^{-1}} = \frac{n_{\alpha}E_1}{R}$$
 [20]

where

$$n_{\alpha}E_1 = E_a \tag{21}$$

Combining Equations 16 and 18 gives a first order differential equation:

$$\frac{d \ln \omega_{\alpha}}{d T^{-1}} - \frac{E_1}{R} \ln \omega_{\alpha} + \frac{E_1}{R} \left(n_{\alpha} + \ln \omega_{\alpha,Arr} \right) = 0$$
 [22]

Expanding the Arrhenius term using Equation 17:

$$\frac{d \ln \omega_\alpha}{d \, T^{-1}} - \frac{E_1}{R} \ln \omega_\alpha + \frac{E_1}{R} \Big(n_\alpha + \ln A_\alpha - \frac{n_\alpha E_1}{RT} \Big) = 0 \qquad [23]$$
 Equation 23 is a first order non homogenous differential equation of the form: y' +ay +bx +c

=0 where y = $\ln \omega_{\alpha}$, x = T⁻¹ and a = $-\frac{E_1}{R}$, b = $-\frac{n_{\alpha}E_1^2}{R^2}$, c = $\frac{E_1}{R}(n_{\alpha} + \ln A_{\alpha})$. The solution is given by

$$\ln \omega_{\alpha} = \ln A_{\alpha} - \frac{n_{\alpha} E_1}{RT} + c_1 e^{\frac{E_1}{RT}}$$
 [24]

As $E_a = n_\alpha E_1$, using Equation 17

As
$$E_a = n_\alpha E_1$$
, using Equation 17
$$\ln A_\alpha - \frac{n_\alpha E_1}{RT} = \ln \omega_{\alpha,Arr}$$
[25] which is substituted into Equation 24:
$$\ln \omega_\alpha = \ln \omega_{\alpha,Arr} + c_1 e^{\frac{E_1}{RT}}$$
[26]

$$\ln \omega_{\alpha} = \ln \omega_{\alpha,Arr} + c_1 e^{\frac{E_1}{RT}}$$
 [26]

To solve for c_1 , a temperature, T_{SA} , where the number of units n_T increases from n_α to $n_\alpha + 1$ is defined. It describes the divergence of ω_{α} from $\omega_{\alpha,Arr}$ by a factor of 1/e:

$$\ln\left(\frac{\omega_{\alpha,Arr}(T_{SA})}{\omega_{\alpha}(T_{SA})}\right) = -c_1 e^{\frac{E_1}{RT_{SA}}} = 1$$
 [27]

This allows us to write c1 as

$$c_1 = -e^{\frac{E_1}{RT}SA}$$
 [28]

and substituting E_1 with E_a/n_α finally gives

$$\ln \omega_{\alpha} = \ln \omega_{\alpha,Arr} - exp\left(\frac{E_{\alpha}}{n_{\alpha}R}\left(\frac{1}{T} - \frac{1}{T_{SA}}\right)\right)$$
 [29]

Assuming the temperature range reaches well into the Arrhenius region (reflected by a linear ln ω_{α} versus 1/T plot) the only parameter which is not directly and uniquely obtained from the data is n_α, which remains the only freely adjustable fit parameter, albeit limited to integer values between 1 and 4 (Table 1). We have presented a form of Equation 29 for polymers but, despite excellent agreement with experimental results, we were not able to rationalize each parameter.43

Results

We tested Equation 29 against experimental data from a wide range of glass formers representing the glassy universe. We used only data which spanned both the high temperature and supercooled regions, giving A_{α} , E_{a} , and T_{SA} experimentally. The impressive agreement is illustrated in Figure 5, with detail on 21 glasses provided in Table 1 (see Figure S1 for individual plots). Classification of glasses is made according to n_{α} in Table 1, which also lists the measured A_{α} , E_a and T_{SA} . We emphasize that T_{SA} uniquely occurs at $n_T = n_{\alpha} + 1$ and was also taken directly from the data (see Figures S2 and S3 for detail on how E_a and T_{SA} ,

respectively, were determined). Selection of n_{α} is not arbitrary; Figure S4 shows an example outcome if n_{α} is selected to be \pm 1 of its optimal value (Table 1) or if T_{SA} is forced to be off by a few degrees from the value read in Figure S3. In contrast, reasonable VFT fits may be obtained with widely different combinations of $\omega_{0,VFT}$, D and T_{0} .

Because T_g in polymers depends on chain length below a certain molecular weight⁴⁵ (ca. 10^4 Daltons), the values of E_a and T_{SA} also depend somewhat on molecular weight. Most of the temperature-controlled glass relaxation in the literature is fit to some reasonable extent by Equation 29. The fidelity of the data is somewhat degraded on transcribing literature plots and a few degrees of error in the temperature measurement near T_{SA} would cause noticeable deviation (for an example see Figure S4B, Supplemental Information).

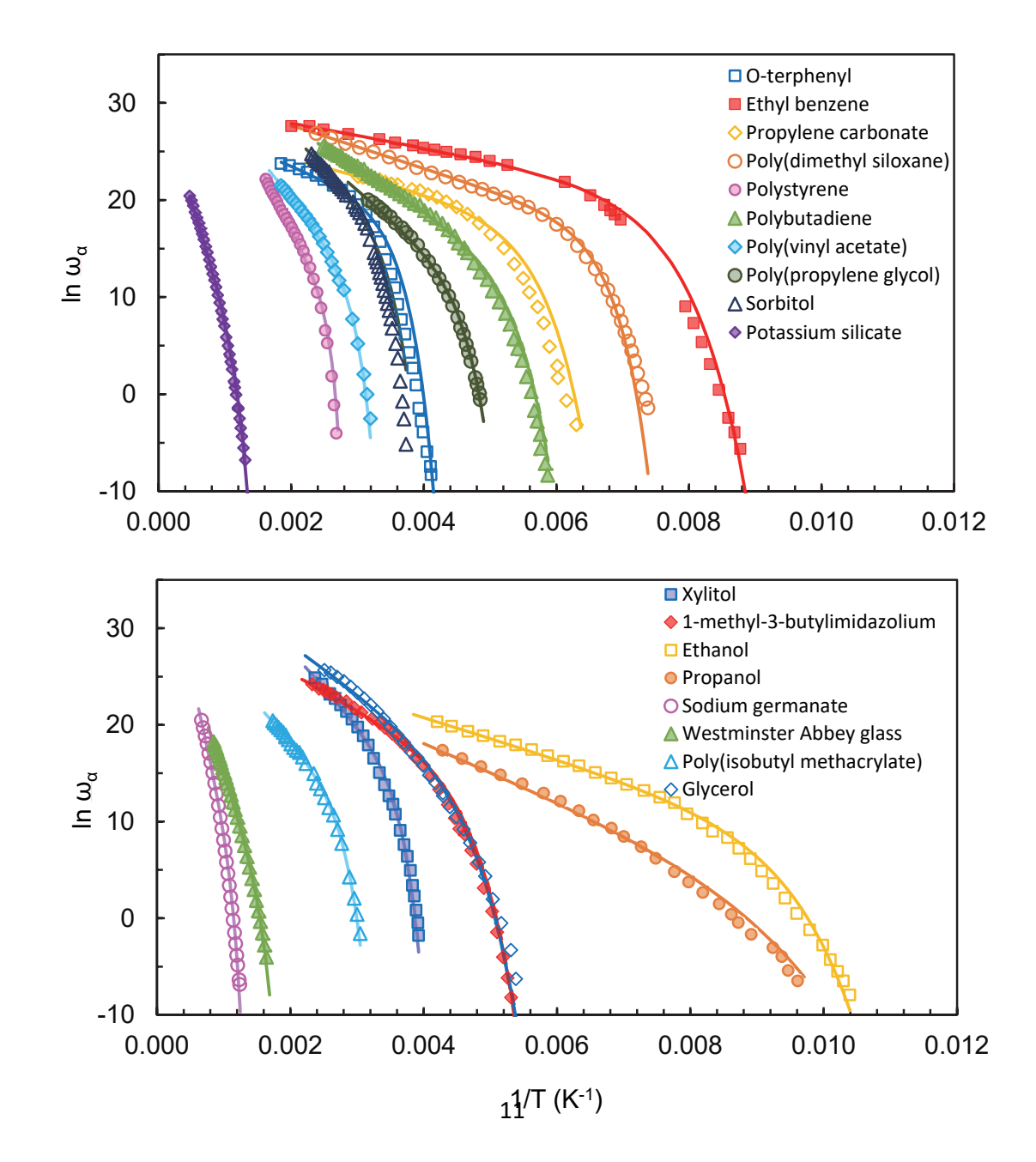
Table 1. Glass formers whose dynamics are reported in Figure 5 and Figure S1 along with their corresponding n_{α} , glass transition temperature (T_g), activation energy (E_a), structural preexponential factor A_{α} , fragility m, T_{SA} and the corresponding references.

E _a (kJ mol ⁻													
Glass Former	n_{α}	T _g (K)	` ¹)	m	n at Tg ^a T _{SA} (K) ^b		A_{α} (s ⁻¹)						
o-terphenyl (OTP) ²⁸	1	240	23.2	81 ²⁷	26 (16)	338 (4)	4.4 x 10 ¹²						
Ethylbenzene ³⁰	1	115	10.5	72°	24 (14)	162 (1)	1.6 x 10 ¹³						
Propylene Carbonate (PC) ¹⁴	1	157	14.3	132 ²⁷	21 (28)	216 (2)	1.1 x 10 ¹²						
Poly(dimethylsiloxane) (PDMS) ³⁰	1	144	19.4	79°	17 (22)	165 (1)	1.2 x 10 ¹⁴						
Polystyrene (PS) ⁴³	2	373	111	105 ⁴³	14 (14)	421 (1)	9.7 x 10 ¹⁸						
Polybutadiene (PB) ⁴⁶	2	174	35.3	84 ^c	17 (16)	224 (2)	4.5 x 10 ¹⁵						
Poly(vinyl acetate) (PVA) ⁴³	2	313	70.6	76 ⁴³	13 (13)	390 (2)	1.5 x 10 ¹⁶						
Poly(isobutyl methacrylate) (PiBM) ⁴³	2	328	61.6	65 ⁴³	13(13)	426 (4)	2.8 x 10 ¹⁴						
Poly(propylene glycol) (PPG) ⁴⁷	2	206	47.9	11 7 ²⁷	13 (19)	249 (2)	4.6 x 10 ¹⁶						
Xylitol ⁴⁸	2	248	61.8	94 ⁴⁸	20 (14)	316 (2)	3.0×10^{18}						
1-methyl-3-butyl-imidazolium ⁴⁹	2	193	30.4	71°	19 (17)	275 (1)	1.6 x 10 ¹⁴						
Ni _{62.4} Nb _{37.6} ⁵⁰	2, 7/4 ^d	945	147	121 ⁵⁰	26 (27)	1380 (5)	1.6 x 10 ¹⁷						
Ethanol⁵¹	2	97	17.7	61 ⁵¹	14 (13)	129 (1)	5.2 x 10 ¹²						
D-Sorbitol ⁴⁸	2	268	66.2	128 ⁴⁸	19 (20)	326 (3)	5.0 x 10 ¹⁸						
Glycerol ⁴⁸	3	186	40.3	57 ⁴⁸	20 (15)	288 (3)	3.4 x 10 ¹⁶						
Pt ₆₀ Ni ₁₅ P ₂₅ ⁵⁰	3, 5/2 ^d	464	62.6	67 ⁵⁰	25 (27)	926 (5)	5.6 x 10 ¹⁵						
Propanol ⁵²	4	106	24.1	40 ²⁷	12 (13)	145 (3)	8.8 x 10 ¹²						

$Pd_{40}Ni_{40}P_{20}{}^{50}$	4, 7/2 ^d	554	104	48 ⁵⁰	18 (20)	1050 (5)	8.3 x 10 ¹⁵
Sodium Germanate ⁵³	4	801	250	46 ⁵³	14 (11)	1099 (5)	4.1 x 10 ¹⁷
Westminster Abbey glass ⁵⁴	4	592	166	42 ⁵⁴	13 (12)	799 (3)	2.0 x 10 ¹⁵
Potassium Silicate ⁵³	4	739	175	33 ⁵³	13 (11)	1162 (5)	1.4 x 10 ¹³

 $^{^{}a}$ n_{Tg} is calculated using Equation 19 at T = T_g and the value in parentheses is estimated using $m = \frac{n_{Tg}E_{a}}{2.3n_{\alpha}RT_{g}}$ and literature values for m (superscripts are references).

 $[^]d$ fractional n_{α}



b± error estimate in parentheses, K

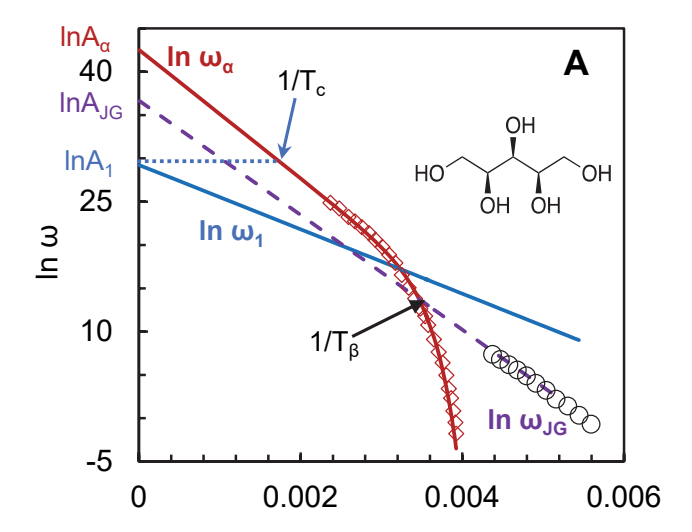
cmeasured from Figure 5

Figure 5. Comparison of Equation 29 with experimental data for different types of glasses as a function of 1/T. The α -relaxation rate, ω_{α} (s⁻¹) of a selection of inorganic, polymer and small molecule glass formers. Symbols are experimental points from the literature. Solid curves are the results of Equation 29 using the measured parameters listed in Table 1. Only n_{α} is freely adjustable (but must be an integer between 1 and 4).

Discussion

Equation 29 relies on a well-accepted TST foundation with the addition of a statistical term $e^{-n_{c(T)}}$, which accounts for deviation from Arrhenius. With the Arrhenius slope, T_{SA} and n_{α} , Equation 29 predicts the entire supercooled region. TST expressions contain a transmission coefficient term, κ , usually assumed to be 1, but is < 1 if some activated complexes do not give rise to products. ⁵⁵ Given the probabilistic derivation of $n_{c(T)}$ it can be thought of as a κ : some groups of n_{α} units have sufficient energy to rearrange but only a fraction $e^{-n_{c(T)}} = \kappa$ actually do so. Eyring's assumption that $\kappa = 1$ for liquids ¹⁶ and glasses ⁵⁶ would thus be correct in the Arrhenius regime far above T_{α} i.e. in the liquid state.

Criteria for whether a secondary relaxation may be considered a "true" β_{JG} , the precursor to the α -relaxation, have been provided by Ngai and coworkers. In broadband dielectric spectroscopy, BDS, for many glasses, β_{JG} shows up as a high frequency wing or shoulder on the much more intense α -relaxation. Deconvolution with arbitrary fitting functions may not provide reliable β_{JG} values. Thus, the use of glass formers with well-distinguished α - and β -peaks in the BDS is preferred, such as the series of polyols reported by Döß et al. Figure 6 shows a examples of relaxation maps for xylitol and sorbitol (n_{α} = 2). The primitive ω_1 rattle of one unit, with an Arrhenius slope -E₁/R, is the fastest relaxation at all T and extrapolates to A_1 at high T. $\omega_{\beta JG}$ with slope - $n_{\alpha}E_1$ /R describes caged relaxation by n_{α} units.



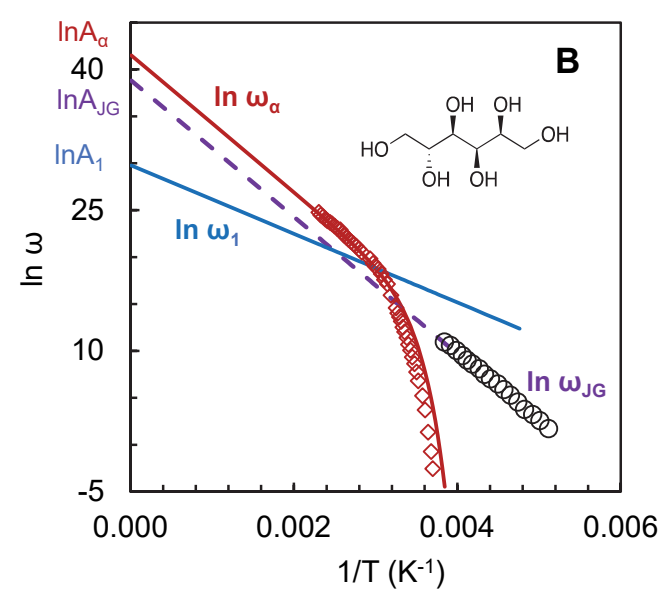


Figure 6. Relaxation map for xylitol (**A**) and sorbitol (**B**). Structural relaxation rate $ω_α$ by cooperative motion among n_T units; open diamonds, experimental $ω_α$ from Döß et al.,⁴⁸ solid line from Equation 29 with parameters in Table 1. Unit rattle $ω_1$ is given in solid blue. $β_{JG}$ relaxation of caged clusters of $n_α$ units in dash ($ω_{βJG}$) from Döß et al. (data: open circles, E_{aJG} = 55.4 kJ and 60.7).⁴⁸ Corresponding intercepts are A_{JG} for the local, caged rattle (8.5 x 10¹⁵ s⁻¹, 9.9 x 10¹⁶ s⁻¹ for xylitol and sorbitol, respectively) and $A_α$ for the structural relaxation. A_1 is the intercept for a single unit rattle assumed to be near the Boson peak, A_{Boson} , = 8.8 x 10¹² s⁻¹ and 5.8 x 10¹² s⁻¹ 60, 61 (although identifying the actual Boson peak from other modes in the ~1 THz range may not be straightforward⁶²). Temperature T_c in panel **A** shows compensation of activation entropy and enthalpy, $E_a = T\Delta S^*_{\text{struct}}$.

The α -relaxation in the Arrhenius region differs from the linear extrapolation of β_{JG} by a factor $\frac{e^{\Delta S_{Struct}^*}}{e^{\Delta S_{JG}^*}}$ (compare Equations 14 and 15). For glasses having n_{α} = 1, the difference is small and may suggest that ω_{α} overlaps in the Arrhenius region with an extrapolated $\omega_{\beta JG}$, as was done in Johari's original paper, which extrapolated a β -relaxation near and below T_g to the liquid state.³³ Usually, $\omega_{\beta JG}$ merges with ω_{α} at temperature T_{β} where $Rn_{c(T=T\beta)} = \Delta S_{struct}^* - \Delta S_{JG}^*$. If ΔS_{JG}^* and ΔS_{struct}^* are small and $A_0 \approx A_{JG} \approx A_{\alpha}$ then $\omega_{\alpha} \approx \omega_{JG}$. This case is more likely to be satisfied when n_{α} = 1. For example, Angell et al. identified a Boson peak in OTP (n_{α} = 1) at 18 cm⁻¹ or 5.4 x 10¹¹ Hz x 2 π = 3.4 x 10¹² s⁻¹ relaxation rate which is close to the A_{α} value in Table 1.⁶³

Several words of caution are needed when making the long extrapolation of $In\omega_{\beta JG}$ to the A_{JG} intercept. First, $\omega_{\beta JG}$ is usually obtained over a narrow range of temperatures in the supercooled and sub- T_g regions, introducing uncertainty in the slope. The data taken from the literature usually shows a slightly different slope between $In\omega_{\alpha}$ and $In\omega_{\beta JG}$. There may be a change in slope for $\omega_{\beta JG}$ as it passes through T_g . However, the β_{JG} data for propanol of Hansen et al. show E_a for $\beta_{JG}=20$ kJ mol⁻¹ compared to an E_a of 24 kJ mol⁻¹ in Table 1. In contrast, the temperature dependence of the β -relaxation time for propanol measured by Caporaletti et al. using both BDS and nuclear resonance time-domain-interferometry, TDI, had an E_a of about 30 kJ mol⁻¹.64 β_{JG} measured via TDI is better decoupled from the α -relaxation.59 Whether the material is at equilibrium when β_{JG} is measured has been addressed. Wagner and Richert noted that isothermal aging of OTP, a widely studied GF, near T_g results in the loss of a peak identified as β_{JG} whereas sorbitol does not suffer from this issue.65

In general, A_{α} for n_{α} > 1 is often at apparently unphysical rates (e.g. 10^{16} - 10^{19} s⁻¹ in Table 1). Even among polymers, there is great variability in A_{α} , while ω_{Boson} for polymers is

clustered around 0.5 THz.⁶⁶ Equations 13 – 15 show the role of activation entropy in TST, whatever the process, be it a unit rattle, an n_{α} rattle, or an n_{α} structural relaxation. ΔS_1^* and ΔS_{JG}^* are likely to be $<\Delta S_{struct}^*$. Qualitatively, for $n_{\alpha}>1$, a *rearrangement* of n_{α} units involves a greater volume than a *rattle*. Since $n_{C(T)} \rightarrow 0$ at high temperature, the difference $ln\omega_{\alpha} - ln\omega_{JG} = (\Delta S_{struct}^* - \Delta S_{JG}^*)/R$. This explains the roughly parallel nature of the $ln\omega_{\alpha}$ and extrapolated $ln\omega_{JG}$ plots at high temperature (Figure 6).

Lawson, in analyzing activated processes in solids, derived an approximate equation for relating the activation entropy to the volume change, ΔV^* , of an activated process⁶⁷

$$\Delta S^* \approx \frac{\delta}{\theta} \Delta V^* \tag{30}$$

Where δ is the isobaric volume coefficient of thermal expansion and θ the isothermal compressibility. Keyes followed with an approximate relationship between activation volume and energy⁶⁸

$$\Delta V^* \approx c\theta \Delta H^*$$
 [31]

Where c is a dimensionless constant. Rault⁶⁹ points out that these lead to

$$\Delta S^* \approx c\delta \Delta H^* \tag{32}$$

and he estimated c to be about 3 in the α -relaxation of a polymer. Equation 32 is a statement of the compensation law or Meyer-Neldel rule, 70 also known as entropy-enthalpy compensation and applies when the energy for an activated process is much larger than the thermal energy kT. 70 Briefly, for an activated process, an increase in enthalpy (thermodynamically unfavorable) is partially compensated by an increase in entropy (favorable). The phenomenon is widely observed in physics 70 and physical (bio)chemistry. The enthalpic part of the activation free energy (bond breaking, separating dipoles, overcoming van der Waals attractions) flowing into a CRR is recovered and redistributed following relaxation. The entropic part is stored as a local elastic deformation. As a consequence of entropy-enthalpy compensation, there should be a critical temperature T_c where $E_a = T_c \Delta S^*_{\text{struct}}$, at which point $In \omega_{\alpha, \text{arr}} = In A_0$. For xylitol this would be at 585 K, shown in Figure 6A assuming $A_0 \approx A_1$.

Polystyrene has the largest A_{α} of the polymers in Table 1, probably a result of the inherent stiffness (long persistence length) of the backbone. From Eq. 15, $lnA_{\alpha}-lnA_0=\Delta S_{struct}^*/R$. For polystyrene, using values of 6.1 x 10⁻⁴ K⁻¹ and 12.1 x 10⁻¹⁰ Pa⁻¹ at 300 °C (well into the Arrhenius regime) for δ and θ , respectively, ⁷³ and $A_0=2.7$ x 10¹² s⁻¹, ⁷⁴ ΔS_{struct}^* is 126 J mol⁻¹ K⁻¹ and ΔV^* is 250 cm³ which is 2.6 molar volumes of styrene repeat units, or about 1.3 styrene from each of the $n_{\alpha}=2$ units rearranging in the Arrhenius region. Assuming this is the minimum free volume needed to rearrange, supplied at T_g by $n_{Tg}=13$ units of persistence length 4 styrene units each, the fractional free volume, v_f , at T_g , is about 2.6/(13 x 4) = 5 %. Depending on the model, estimates of v_f for polystyrene at T_g range from about 2.5 % (Doolittle model^{7,37,38}) to 11 % (White and Lipson using a PVT model³⁴) to 12 % (from positron lifetime spectroscopy⁷⁵).

Relaxation plots in GFs are known to exhibit a thermodynamic scaling^{8,57} between density, ρ (controlled by pressure), and temperature, where ω_{α} is a function of a single scaling variable T/ ρ^{γ} and γ depends on the GF⁷⁶ In select cases, for small van der Waals GFs such as OTP and PC, the entire relaxation spectrum in BDS follows this scaling.⁸ Such isochronal superposition (IS) could only occur if $e^{\Delta S_{struct}^*} \approx e^{\Delta S_{fg}^*}$ i.e. the activation volumes of β_{JG} and ω_{α} are similar (according to Equation 30). In addition, the ω_{α} broad band spectra at different temperatures superimpose with frequency shifting (time-temperature superposition), e.g. for OTP.⁷⁶ These small, van der Waals GFs are likely to have n_{α} = 1. Niss and Hecksher⁷⁶ point out that polymers ironically do not show TTS over the entire BDS response. This is because n_{α} for polymers usually = 2.

As with most models in GF dynamics, it is assumed that there are no significant changes in the mechanism of relaxation over the temperature range from liquid to T_g . E_a is read from relaxation data taken at temperatures well above T_g . Clearly, GFs which are not stable at these elevated temperatures do not give reliable E_a . Nevertheless, there are numerous GFs which remain stable in the Arrhenius region. For these, the main assumption is that the activation energy does not change significantly in the supercooled region. Support

for this assumption is given by the correlation coefficients in the respective Arrhenius plots in Figure S1. The n_{α} = 1 GFs are fragile and potentially the most troublesome, since data for their Arrhenius regions is limited and more scattered (Figure S1). The fit of Equation 29 with the n_{α} = 1 data (Figure 5) is least satisfactory. While PDMS and EB are reasonably represented by Equation 29, the data for OTP and PC suggest that fragile glasses are more susceptible to errors in E_a and T_{SA}.

A strong change in E_a approaching T_g (see Figure 2) is a central feature of some analyses, such as those of Kivelson et al.²⁹ and Schmidtke et al.,³⁰ who decompose E_a into a temperature independent part (i.e. taken from the Arrhenius region) and a temperature dependent cooperative part, which grows approaching T_g . We stress that this is quite different from the path taken in the present work, although the $e^{-Ea/RT}$ and $e^{-n(T)}$ terms could be considered to be two barriers: one thermodynamic and one kinetic.

Metallic alloys. Many compositions of metal alloys exhibit glass forming behavior. Three of these bulk metallic glasses were analyzed using Equation 29. Figure 7 shows that the selection of an integral value for n_{α} did not lead to satisfactory fits for the T_{SA} read from the data. An arbitrary T_{SA} would provide an acceptable fit, but a fractional n_{α} (n_{α} = 5/2, 7/2, 7/4) would preserve the T_{SA} prescribed by the data (Supplementary Information Figure S3). The physical significance, if there is one, of fractional n_{α} for metals is not yet clear, but could be related to the nature of metallic binding.

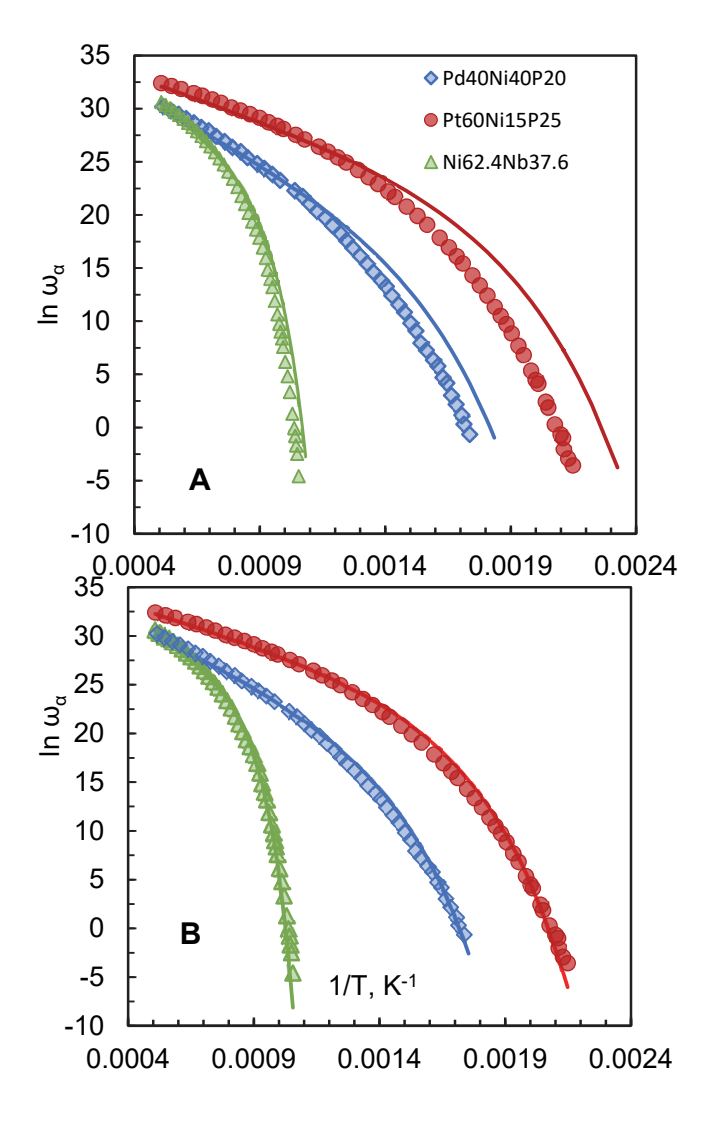


Figure 7. Relaxation in three metallic alloys. Panel **A**: with integer n_{α} values from Table 1. **B** with fractional n_{α} values shown in Table 1. E_a , A_{α} , and T_{SA} are the same for both panels, listed in Table 1.

Classes of glasses. Classification of glasses is typically done by comparing the extent to which their dynamics deviate from high-temperature Arrhenius using a steepness index or kinetic fragility, m, at T_q , 27

$$m = -\left|d\log_{10}\omega_{\alpha}/d\left(T_g/T\right)\right|_{T=T_g}$$
 [33]

Using Eqs. 16 and 19, the fragility and n_{α} are related by $m=\frac{n_{T_g}E_a}{2.3n_{\alpha}RT_g}=\frac{n_{T_g}E_1}{2.3RT_g}$

$$m = \frac{n_{T_g} E_a}{2.3 n_{\alpha} R T_g} = \frac{n_{T_g} E_1}{2.3 R T_g}$$
 [34]

which provides a quick estimate of the n_α class using literature T_g , m and E_a without fitting the data over all temperatures. The origin of fragility is a perplexing issue in glass physics. From Equation 34, the origin of fragility and the reasons for the wide range of values of m are clear: it is a combination of three parameters. n_{Tg} has a lower spread of values (about a factor of two) than does T_g or E_1 . Some of the glass formers with a large E_a actually have much lower E_1 if n_α is 4. Thus, the silicate glasses, with $n_\alpha = 4$ and high T_g s, push fragility lower. Small molecules with low T_g and van der Waals interactions (where $n_\alpha = 1$) tend toward the upper half of fragilities.

Table 1 shows reasonable agreement between n_{Tg} (n at T = T_g) estimated with Equation 34 using the literature m values and those calculated using Equation 19. The actual T_g is not predicted from the equations herein, although it can be predicted with the locally correlated lattice (LCL)²¹ model, which is a first-principles thermodynamic treatment of PVT data. The LCL model frees itself of the constraint arbitrarily placed on Doolittle's free volume to make it follow VFT response. ²¹

Supercooled liquids approach icosahedral ordering⁷⁷ near T_g and atomistic models show such ordering improves with observation time. 78 In fact, the CRR is only compact at Tg and, if quasi-icosahedral, would imply n_{Tg} of about 13, representing a central unit surrounded by 12 nearest neighbors. The configuron percolation model⁷⁹ supports conclusions by Wendt and Abraham⁸⁰ that packing saturation of the first shell by nearest neighbors at T_a is predicted by analysis of the pair distribution function (PDF). Example X-ray scattering studies on PDFs of metallic glasses show a coordination number of about 12.381 and 12.682 From Table 1, many n_{Tq} are clustered at around 13 but this is not universal, probably reflecting anisotropy83 in the interaction environment of a unit, such as the hydrogen bonding patterns in xylitol and glycerol. Note that polymers are structurally anisotropic (they are chains) but each moving unit might experience the same interaction environment.⁴³ n_{Tg} is sensitive to the slope of the fit at T_g, which is least satisfactory for the OTP fit. The measured slope from the OTP data near T_g (see Figure S1) gives $n_{Tg} = 13$. Overall, the answer to "what happens at T_g ?" is, for many systems, "that is the lowest temperature where about 13 neighboring units with a nearicosahedral interaction environment can cooperatively rearrange within τ_1 to provide the free volume that allows n_{α} units to rearrange simultaneously." n_{Tq} may be larger or smaller if the environment does not have icosahedral symmetry, or the units themselves adopt different ordering as required, for example, by hydrogen bonding. Dynamic modeling that starts with spherically symmetric units (e.g. beads) would be expected to achieve idealized short-range ordering approaching close packing.

If cooperativity in the first coordination shell is saturated at T_g , what happens when the glass is further cooled? The next-nearest neighbor shell must participate in $n_{c(T)}$. Modeling of amorphous materials by Mercier and Levy⁸⁴ suggests that the packing goes from 13 units to 43 if the next coordination shell is included (for spherical units). One can expect another glass transition at a lower temperature where the entire shell of next-nearest neighbors must also cooperatively rearrange. The changes between coordination shells probably underly second-order like transitions such as a change in expansion coefficient and a step in heat capacity at T_g . Equation 29 is not extended below T_g as we have not analyzed sufficient data to know

whether E_1 is preserved below T_g . There is evidence that below T_g the relaxation response is Arrhenius with a much higher apparent Ea than that above TSA. 85 However, data from Hecksher et al. reveals continuing curvature on a $\text{In}\omega_a$ versus 1/T plot below T_g . ¹⁰ We note that for many GFs, E_{a,apparent} in the T_g region is about a factor of 13/n_α larger than E_a from the hightemperature Arrhenius region, as implied by Equation 16.

The physical size of n_{Tg} units is reasonably consistent with experiment. For example if the actual unit in polystyrene is a persistence length of 1 nm which is 1/0.25 = 4 styrene repeat units and there are 13 of these at T_g , the mass of the CRR is 4 x 13 x 104 g mol⁻¹/6.02 x 10^{23} mol^{-1} = 9.0 x 10⁻²¹ g or 9.0 x 10⁻²⁰ cm³ assuming a density of 1 g cm⁻³ for a size of 2.1 nm, compared to 3.0 nm estimated by Hempel et al.86

Shift Factors. Equation 29 can be rearranged into classical shift factors using the parameters E_a , T_{SA} and n_α (Section S1). In the broadly-used concept of time-temperature superposition, TTS, a shift factor a_T is employed to shift dynamic responses taken at different temperatures and is the ratio between their frequencies, $\frac{\omega_{T_1}}{\omega_{T_2}}$. A typical expression for shift factors in polymers is that of Williams, Landel and Ferry (WLF): $\log 10(a_T) = \frac{-c_1(T_1-T_2)}{c_2+T_1-T_2} \qquad [35]$ where c₁ and c₂ are two empirical (freely adjustable) fit constants.⁸⁷ Using the appropriate

$$\log 10(a_T) = \frac{-c_1(T_1 - T_2)}{c_2 + T_1 - T_2}$$
 [35]

substitutions (Section S1) and Equation 29, we obtain the following:

$$\ln a_T = \frac{E_a}{R} \left(\frac{1}{T_2} - \frac{1}{T_1} \right) + e^{\frac{-C}{T_{SA}}} \left(e^{\frac{C}{T_2}} - e^{\frac{C}{T_1}} \right)$$
 [36]

where $C = E_a/n_\alpha R$. This relationship shows there are two components to the shift factor; the first term on the right represents the Arrhenius response for n_{α} units. The second term includes the probability factor when $n_T > n_\alpha$. The shift factor can then be written as: $a_T = a_A \times a_P$ where a_A is due to the Arrhenius shift of n_α units and a_P is due to the probability factor $e^{-n_{c(T)}}$ for additional n_{c(T)} units imposed by limited free volume. Figure 8 compares shift factors obtained using the WLF equation and Equation 36 for poly(isobutyl methacrylate).

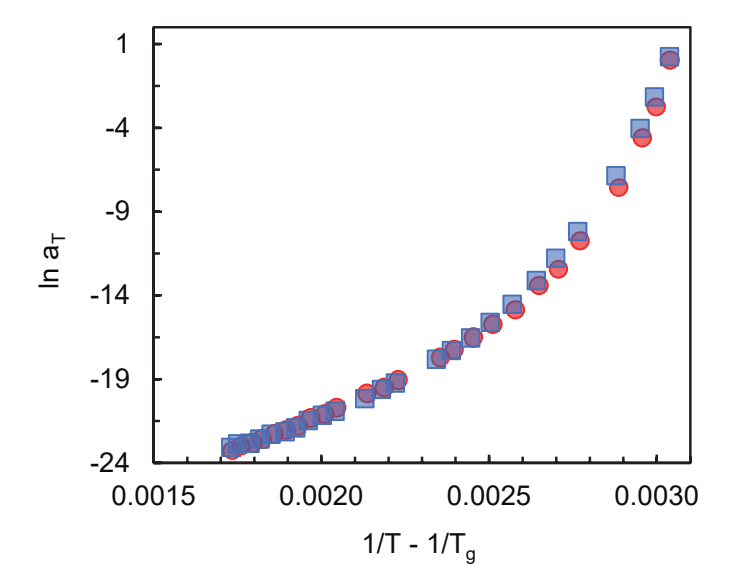


Figure 8. Example of shift factor calculations. The shift factor a_T for poly(isobuty) methacrylate) calculated using WLF Equation 35 (red circles) and Equation 36 (blue squares). The empirical WLF fit constants were: c_1 = 12.4 and c_2 = 57 °C and T_2 = T_g . Values for n_α , E_a and T_{SA} used for Equation 36 are given in Table 1.

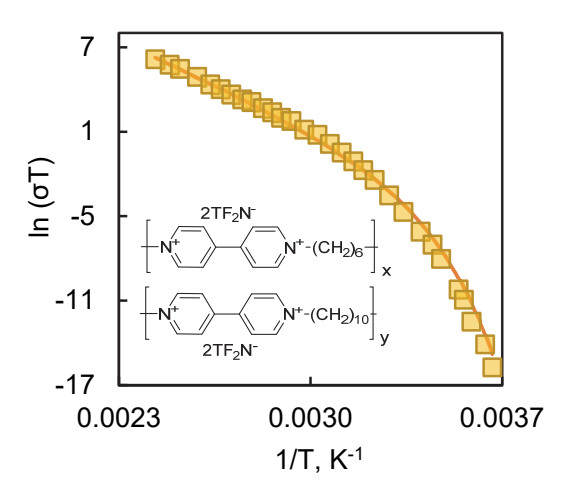
Crossover Temperatures. While the WLF equation is mathematically equivalent to the VFT equation, it cannot be superimposed on Equations 29 or 36. The WLF and VFT equations are often unable to fit *both* the near-T_g *and* the Arrhenius regions (see examples in Figure S5, Supplementary Information). Equation 29, in contrast, can describe the relaxation across wide ranges of temperatures. Equation 29 handily avoids the controversy of a temperature at which ω_α would diverge (the Vogel temperature, T_0 , section S1), close to the temperature T_K at which the entropy of a glass would be equal to the entropy of its crystalline state. 88 This divergence is also avoided by many other descriptions of glass relaxation which use characteristic temperatures greater than $T_g.^1$ Such crossover temperatures define the point of departure from Arrhenius into supercooled behavior, much like T_{SA} . Stickel et al. presented way to emphasize the crossover region more sharply. 14 The resulting Stickel temperature, T_B , is in the vicinity of T_{SA} (e.g. T_B = 243 K for PPG 12) or not very close (e.g. T_B = 296 K for OTP 12). Martinez-Garcia et al. compared T_B with the critical temperature, T_C , from mode coupling theory and found T_C to be in the vicinity of $T_B.^{12}$

Cooperative Dynamics in Ion-Polymer Coupled Systems. Many phenomena are coupled to structural dynamics.^{89, 90} For example, ion conductivity in polymers is usually shown to be coupled to the dynamics of the polymer host.^{91, 92} The dependence of conductivity on temperature for an example ion conducting polymer is modeled well by adapting Equation 29 using n_{α} = 2 (Figure 9 and Supplemental Information Section S2).

$$\ln \sigma_T T = \ln \sigma_{T,Arr} T - exp\left(\frac{E_a}{2R}\left(\frac{1}{T} - \frac{1}{T_{SA}}\right)\right)$$
 [37]

We calculated n_{Tg} to be 13. For a particular set of variables in Eq. 37, anything that increases the activation entropy will increase σ .

Figure 9. Conductivity plot of bis(trifluoromethylsulfonyl)imide, 93 TF₂N-, in a single-ion



polyviologen conductor (PV_C₆/C₁₀, structure given in inset). Solid line is Equation 37 using n_{α} = 2, measured E_a = 75.2 kJ mol⁻¹, measured T_{SA} = 317 K.

This system is a single ion conductor, where the TF_2N^- counterion is free to transport charge through the bulk of the material, whereas the positive charge resides on the polymer chain and is thus not free to diffuse.⁹³ The conductivity σT is proportional to the ion diffusion coefficient, D_T . The good agreement given in Figure 9 supports the idea that the transport of ions is coupled to the dynamics of the host polymer. Some ion transport below T_g is claimed to be decoupled from polymer dynamics.⁹⁴ This may be true for the α -relaxation but there must still be some phonon-type of contribution from the matrix in which the ion is embedded. The "unphysically high prefactors" up to 10^{28} s⁻¹ for ion transport in polymer electrolytes recently highlighted by Gainaru et al.⁹⁴ must include a significant ΔS^* .

Cooperative Dynamics in Spin Systems. Equation 29 broadly describes a quenched state where increasing numbers of cooperatively interacting units are obtained at lower temperatures with the emergence of heterogenous dynamic length scales. Spin glasses and ferromagnetic relaxors potentially fit this description. For example, Figure 10 shows relaxation dynamics for perovskite ferroelectrics PLZT ($Pb_{1-x}La_x(Zr_{1-y},Ti_y)_{1-x/4}O_3$) and PMN-PT⁹⁵ ($Pb(Mg_{1/3}Nb_{2/3})O_3$)-PbTiO₃ represented by Equation 29 with respective n_α values of 0.5 and 2.

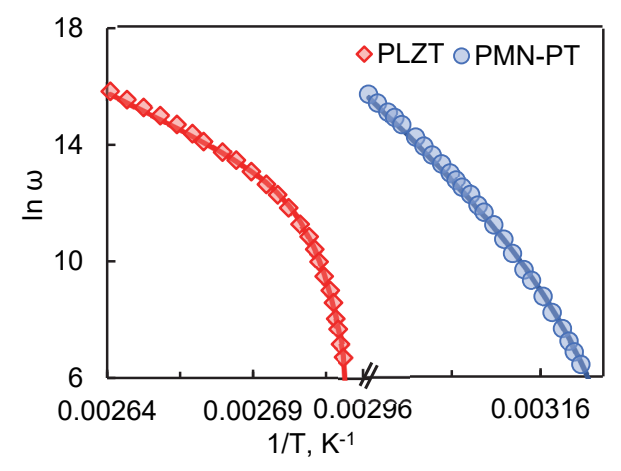


Figure 10. The frequency of ferroelectric relaxors versus 1/T. Pb(Mg_{1/3}Nb_{2/3})O₃ – PbTiO₃ (PMN-PT, \circ): n_{α} = 2, experimental E_a = 229 kJ mol⁻¹, measured T_{SA} = 319 K; and Pb_(1-x)La_x(Zr_{1-y}Ti_y)_{1-x/4}O₃ (PLZT, \diamond): n_{α} = 0.5, experimental E_a = 422 kJ mol⁻¹, measured T_{SA} = 369 K . Points are experimental data from ref ⁹⁵; solid line from Equation 29.

In the case of electric (or magnetic) dipoles we interpret an n_{α} of 0.5 to represent one dipole switching direction from +1 to -1 (rather than +1 to 0).

Conclusions

We have presented an equation based on measurable parameters that allows quantitative description and classification of GF dynamics according to the minimum number of units that must rearrange simultaneously. The motion of units has been broken down into those occurring simultaneously (concerted/correlated) and those occurring within interval τ_1 . n_α represents the minimum cluster size of rearranging units, observed at high temperatures. These units escape their cages simultaneously with frequency ω_α , but only if there is enough free volume to do so. Otherwise, one observes a correlated rattle at ω_{JG} , the JG β -relaxation. ω_{JG} accounts for the Arrhenius slope of ω_α at high temperature. Additional spatiotemporal restrictions are encountered as the temperature drops, limiting the free volume. A probability term incorporates dynamic heterogeneity and deviation from Arrhenius due to a growing length scale of cooperativity as the glass cools.

The only freely-adjustable fitting term is n_{α} , which, for all glass formers except metal alloys, is an integer between 1 and 4. A mixture of kinetics and thermodynamics is inherent to Equation 12. The E_a term refers to the steady-state (equilibrium) Boltzmann distribution of the number of n_{α} units with energy sufficient to simultaneously escape their cages. The $n_{c(T)}$ term is a result of additional kinetic restrictions. Though our approach can be classified as a free volume argument, the actual free volume is not needed. Neither the free volume at T_g , nor T_g itself is specified. In fact, the most important temperature regime is around T_{SA} because it provides E_a and T_{SA} . With the Arrhenius slope, T_{SA} , and n_{α} , the entire supercooled regime between T_{SA} and T_g is predicted with reasonable accuracy. Using the TST approach allows the apparently unphysical prefactors found in equations representing many GF dynamics to be rationalized in terms of an activation entropy contribution, which provides an activation volume.

According to the n_{α} classification system, small van der Waals GFs have n_{α} = 1 and most polymers have n_{α} = 2. An exception is PDMS, which has a highly flexible backbone and a low barrier to switching between *gauche* and *trans* Si-O-Si configurations. The hydrogen bonded molecules studied here exhibit n_{α} from 2 to 4. Oxide glasses were n_{α} = 4.

The results are entirely consistent with work attributing certain β -relaxations to caged precursors, $^{8, 35, 96}$ which are unleashed above T_g as groups of n_α units assisted by cooperative motions among $n_\alpha+n_{c(T)}$ units. Extrapolations of ω_α to the liquid state (i.e. $T>T_{SA}$) provide deep implications on how liquids flow. For example, substances with $n_\alpha>1$ move in clusters of n_α , not as individual units. Knowing n_α should improve molecular simulations and vice versa. The persistence length exchange mechanism suggested for polymers (Figure 3), if it holds up under scrutiny from molecular dynamics simulations, may be universal for most polymers. The $n_\alpha=2$ found for ionic liquids may also be universal, and may represent the place exchange of two neighboring like-charged ions to preserve the local electrostatic field. The possibility that metals and spin systems may exhibit fractional n_α should be further investigated.

While Equation 29 brings much-needed simplicity⁷⁶ to a quantitative relationship for glassy dynamics *versus* temperature, many challenges remain, including developing a more sophisticated picture of both the nature of a "unit", which is not necessarily spherical, and its interaction environment. Some assumptions have been made which are not strictly valid. For example, whatever high frequency mode actually represents A_1 shows slight temperature dependence.⁶² The activation barrier E_1 (E_a) is also likely not constant over the supercooled region, though any changes may be small enough for the overall model to remain valid.

Author Information

Corresponding Author

J.B. Schlenoff - Department of Chemistry and Biochemistry, The Florida State University, Tallahassee, Florida 32306-4390, United States. Email: jschlenoff@fsu.edu
Authors

K. Akkaoui - Department of Chemistry and Biochemistry, The Florida State University, Tallahassee, Florida 32306-4390, United States

Acknowledgments

This work was supported by the National Science Foundation (grants DMR-1809304 and DMR-2103703).

Conflict of Interest

The authors have no conflicts to disclose.

Author Contributions

Joseph Schlenoff: Conceptualization (lead), supervision, review, writing, editing, analysis. **Khalil Akkaoui:** conceptualization, review, writing, editing, analysis.

Supplementary Information

Individual relaxation plots of the glass formers transcribed from the literature, along with E_a , A_α and T_{SA} ; comparison with VFT and WLF equations; VFT fit for 4 glasses; Equation 29 adapted for ionic conductivity.

References

- ¹S. A. Kivelson, and G. Tarjus, "In search of a theory of supercooled liquids," *Nature Materials* **7**, 831-833 (2008).
- ² P. G. Debenedetti, and F. H. Stillinger, "Supercooled liquids and the glass transition," *Nature* **410**, 259-267 (2001).
- ³ L. Berthier, G. Biroli, J.-P. Bouchaud, L. Cipelletti, D. E. Masri, D. L'Hôte, F. Ladieu, and M. Pierno, "Direct experimental evidence of a growing length scale accompanying the glass transition," *Science* **310**, 1797-1800 (2005).
- ⁴ L. M. C. Janssen, "Mode-coupling theory of the glass transition: A primer," *Frontiers in Physics* **6:97**, (2018).

- ⁵ J. Málek, "Structural relaxation rate and aging in amorphous solids," *The Journal of Physical Chemistry C* **127**, 6080-6087 (2023).
- ⁶ H. Solunov, "On measuring the characteristic length of the cooperative molecular dynamics in the glass-forming liquids," *J. Phys.: Conf. Ser.* **1186**, 012008 (2019).
- ⁷ B. A. Pazmiño Betancourt, P. Z. Hanakata, F. W. Starr, and J. F. Douglas, "Quantitative relations between cooperative motion, emergent elasticity, and free volume in model glass-forming polymer materials," *Proceedings of the National Academy of Sciences* **112**, 2966-2971 (2015).
- ⁸ K. Ngai, J. Habasaki, D. Prevosto, S. Capaccioli, and M. Paluch, "Thermodynamic scaling of α -relaxation time and viscosity stems from the Johari-Goldstein β-relaxation or the primitive relaxation of the coupling model," *The Journal of Chemical Physics* **137**, 034511 (2012).
- ⁹ H. Tanaka, T. Kawasaki, H. Shintani, and K. Watanabe, "Critical-like behaviour of glass-forming liquids," *Nature Materials* **9**, 324-331 (2010).
- ¹⁰ T. Hecksher, A. I. Nielsen, N. B. Olsen, and J. C. Dyre, "Little evidence for dynamic divergences in ultraviscous molecular liquids," *Nature Physics* **4**, 737-741 (2008).
- ¹¹ J. C. Martinez Garcia, J. L. Tamarit, and S. J. Rzoska, "Enthalpy space analysis of the evolution of the primary relaxation time in ultraslowing systems," *The Journal of Chemical Physics* **134**, 024512 (2011).
- ¹² J. C. Martinez-Garcia, J. Martinez-Garcia, S. J. Rzoska, and J. Hulliger, "The new insight into dynamic crossover in glass forming liquids from the apparent enthalpy analysis," *The Journal of Chemical Physics* **137**, 064501 (2012).
- ¹³ Q. Gao, and Z. Jian, "Fragility and Vogel-Fulcher-Tammann parameters near glass transition temperature," *Mater Chem Phys* **252**, 123252 (2020).
- ¹⁴ F. Stickel, E. W. Fischer, and R. Richert, "Dynamics of glass-forming liquids. II. Detailed comparison of dielectric relaxation, DC-conductivity, and viscosity data," *The Journal of Chemical Physics* **104**, 2043-2055 (1996).
- ¹⁵ V. N. Novikov, and A. P. Sokolov, "Temperature dependence of structural relaxation in glass-forming liquids and polymers," *Entropy* **24**, 1101 (2022).
- ¹⁶ H. Eyring, "Viscosity, plasticity, and diffusion as examples of absolute reaction rates," *The Journal of Chemical Physics* **4**, 283-291 (1936).
- ¹⁷ I. Avramov, and A. Milchev, "Effect of disorder on diffusion and viscosity in condensed systems," *Journal of Non-Crystalline Solids* **104**, 253-260 (1988).
- ¹⁸ P. Hrma, P. Ferkl, and A. A. Kruger, "Arrhenian to non-Arrhenian crossover in glass melt viscosity," *Journal of Non-Crystalline Solids* **619**, 122556 (2023).
- ¹⁹ P. B. Macedo, and T. A. Litovitz, "On the relative roles of free volume and activation energy in the viscosity of liquids," *The Journal of Chemical Physics* **42**, 245-256 (2004).
- ²⁰ M. H. Cohen, and D. Turnbull, "Molecular transport in liquids and glasses," *The Journal of Chemical Physics* **31**, 1164-1169 (2004).
- ²¹ J. C. Mauro, Y. Yue, A. J. Ellison, P. K. Gupta, and D. C. Allan, "Viscosity of glass-forming liquids," *Proceedings of the National Academy of Sciences* **106**, 19780-19784 (2009).
- ²²S. Waterton, "The viscosity-temperature relationship and some inferences on the nature of molten and of plastic glass," *J. Soc. Glass Technol* **16**, 244-247 (1932).
- ²³ G. Adam, and J. H. Gibbs, "On the temperature dependence of cooperative relaxation properties in glass-forming liquids," *The Journal of Chemical Physics* **43**, 139-146 (1965).
- ²⁴ G. P. Johari, "A resolution for the enigma of a liquid's configurational entropy-molecular kinetics relation," *The Journal of Chemical Physics* **112**, 8958-8969 (2000).

- ²⁵ L. Berthier, M. Ozawa, and C. Scalliet, "Configurational entropy of glass-forming liquids," *The Journal of Chemical Physics* **150**, 160902 (2019).
- ²⁶ S. Tatsumi, S. Aso, and O. Yamamuro, "Thermodynamic study of simple molecular glasses: Universal features in their heat capacity and the size of the cooperatively rearranging regions," *Physical Review Letters* **109**, 045701 (2012).
- ²⁷ R. Böhmer, K. Ngai, C. A. Angell, and D. Plazek, "Nonexponential relaxations in strong and fragile glass formers," *The Journal of Chemical Physics* **99**, 4201-4209 (1993).
- ²⁸ R. Greet, and D. Turnbull, "Glass transition in o-terphenyl," *The Journal of Chemical Physics* **46**, 1243-1251 (1967).
- ²⁹ D. Kivelson, S. A. Kivelson, X. Zhao, Z. Nussinov, and G. Tarjus, "A thermodynamic theory of supercooled liquids," *Physica A: Statistical Mechanics and its Applications* **219**, 27-38 (1995).
- ³⁰ B. Schmidtke, M. Hofmann, A. Lichtinger, and E. A. Rössler, "Temperature dependence of the segmental relaxation time of polymers revisited," *Macromolecules* **48**, 3005-3013 (2015).
- ³¹ J.-H. Hung, T. K. Patra, V. Meenakshisundaram, J. H. Mangalara, and D. S. Simmons, "Universal localization transition accompanying glass formation: Insights from efficient molecular dynamics simulations of diverse supercooled liquids," *Soft Matter* **15**, 1223-1242 (2019).
- ³² M. D. Ediger, M. Gruebele, V. Lubchenko, and P. G. Wolynes, "Glass dynamics deep in the energy landscape," *The Journal of Physical Chemistry B* **125**, 9052-9068 (2021).
- ³³ G. P. Johari, "Intrinsic mobility of molecular glasses," *The Journal of Chemical Physics* **58**, 1766-1770 (1973).
- ³⁴ G. P. Johari, and M. Goldstein, "Viscous liquids and the glass transition. II. Secondary relaxations in glasses of rigid molecules," *The Journal of Chemical Physics* **53**, 2372-2388 (1970).
- ³⁵ S. Capaccioli, M. Paluch, D. Prevosto, L.-M. Wang, and K. Ngai, "Many-body nature of relaxation processes in glass-forming systems," *The Journal of Physical Chemistry Letters* **3**, 735-743 (2012).
- ³⁶ C. Chang, H. Zhang, R. Zhao, F. Li, P. Luo, M. Li, and H. Bai, "Liquid-like atoms in dense-packed solid glasses," *Nature Materials* **21**, 1240-1245 (2022).
- ³⁷ A. K. Doolittle, "Studies in Newtonian flow. II. The dependence of the viscosity of liquids on free-space," *Journal of Applied Physics* **22**, 1471-1475 (1951).
- ³⁸ D. Turnbull, and M. H. Cohen, "Free-volume model of the amorphous phase: Glass transition," *The Journal of Chemical Physics* **34**, 120-125 (1961).
- ³⁹ R. P. White, and J. E. G. Lipson, "Polymer free volume and its connection to the glass transition," *Macromolecules* **49**, 3987-4007 (2016).
- ⁴⁰ I. Farnan, and J. F. Stebbins, "High-temperature silicon-29 NMR investigation of solid and molten silicates," *Journal of the American Chemical Society* **112**, 32-39 (1990).
- ⁴¹ W. K. Kegel, van Blaaderen, and Alfons, "Direct observation of dynamical heterogeneities in colloidal hard-sphere suspensions," *Science* **287**, 290-293 (2000).
- ⁴² W.-S. Xu, J. F. Douglas, and Z.-Y. Sun, "Polymer glass formation: Role of activation free energy, configurational entropy, and collective motion," *Macromolecules* **54**, 3001-3033 (2021).
- ⁴³ J. B. Schlenoff, and K. Akkaoui, "Dissecting dynamics near the glass transition using polyelectrolyte complexes," *Macromolecules* **54**, 3413-3422 (2021).
- ⁴⁴ M. Zhang, Y. Chen, and L.-h. Dai, "Universal scaling in the temperature-dependent viscous dynamics of metallic glasses," *The Journal of Physical Chemistry B* **125**, 3419-3425 (2021).

- ⁴⁵ C. Roland, and R. Casalini, "Temperature dependence of local segmental motion in polystyrene and its variation with molecular weight," *The Journal of Chemical Physics* **119**, 1838-1842 (2003).
- ⁴⁶ M. Hofmann, N. Fatkullin, and E. A. Rössler, "Inconsistencies in determining the entanglement time of poly(butadiene) from rheology and comparison to results from field-cycling NMR," *Macromolecules* **50**, 1755-1758 (2017).
- ⁴⁷ A. Schönhals, H. Goering, and C. Schick, "Segmental and chain dynamics of polymers: From the bulk to the confined state," *Journal of Non-Crystalline Solids* **305**, 140-149 (2002).
- ⁴⁸ A. Döß, M. Paluch, H. Sillescu, and G. Hinze, "Dynamics in supercooled polyalcohols: Primary and secondary relaxation," *The Journal of Chemical Physics* **117**, 6582-6589 (2002).
- ⁴⁹ A. Rivera, A. Brodin, A. Pugachev, and E. Rössler, "Orientational and translational dynamics in room temperature ionic liquids," *The Journal of Chemical Physics* **126**, 114503 (2007).
- ⁵⁰ A. Takeuchi, H. Kato, and A. Inoue, "Vogel–Fulcher–Tammann plot for viscosity scaled with temperature interval between actual and ideal glass transitions for metallic glasses in liquid and supercooled liquid states," *Intermetallics* **18**, 406-411 (2010).
- ⁵¹ R. Brand, P. Lunkenheimer, U. Schneider, and A. Loidl, "Excess wing in the dielectric loss of glass-forming ethanol: A relaxation process," *Physical Review B* **62**, 8878-8883 (2000).
- ⁵² C. Hansen, F. Stickel, T. Berger, R. Richert, and E. W. Fischer, "Dynamics of glass-forming liquids. III. Comparing the dielectric α -and β -relaxation of 1-propanol and o-terphenyl," *The Journal of Chemical Physics* **107**, 1086-1093 (1997).
- ⁵³ D. S. Sanditov, and M. I. Ojovan, "On relaxation nature of glass transition in amorphous materials," *Physica B: Condensed Matter* **523**, 96-113 (2017).
- ⁵⁴ O. Gulbiten, J. C. Mauro, X. Guo, and O. N. Boratav, "Viscous flow of medieval cathedral glass," *Journal of the American Ceramic Society* **101**, 5-11 (2018).
- ⁵⁵ K. J. Laidler, and M. C. King, "Development of transition-state theory," *The Journal of Physical Chemistry* **87**, 2657-2664 (1983).
- ⁵⁶ G. L. Faerber, S. W. Kim, and H. Eyring, "Viscous flow and glass transition temperature of some hydrocarbons," *The Journal of Physical Chemistry* **74**, 3510-3518 (1970).
- ⁵⁷ K. L. Ngai, and M. Paluch, "Classification of secondary relaxation in glass-formers based on dynamic properties," *The Journal of Chemical Physics* **120**, 857-873 (2004).
- 58 U. Schneider, R. Brand, P. Lunkenheimer, and A. Loidl, "Excess wing in the dielectric loss of glass formers: A Johari-Goldstein β-relaxation?" *Physical Review Letters* **84**, 5560-5563 (2000).
- ⁵⁹ K. L. Ngai, "Microscopic understanding of the Johari-Goldstein β-relaxation gained from nuclear γ-resonance time-domain-interferometry experiments," *Phys Rev E* **104**, 015103 (2021).
- ⁶⁰ Y. Osamu, H. Kouji, M. Takasuke, T. Kiyoshi, T. Itaru, and K. Toshiji, "Boson peaks of glassy mono- and polyalcohols studied by inelastic neutron scattering," *Journal of Physics: Condensed Matter* **12**, 5143 (2000).
- ⁶¹ L. Hong, P. D. Gujrati, V. N. Novikov, and A. P. Sokolov, "Molecular cooperativity in the dynamics of glass-forming systems: A new insight," *The Journal of Chemical Physics* **131**, (2009).
- ⁶² M. González-Jiménez, T. Barnard, B. A. Russell, N. V. Tukachev, U. Javornik, L.-A. Hayes, A. J. Farrell, S. Guinane, H. M. Senn, A. J. Smith, M. Wilding, G. Mali, M. Nakano, Y. Miyazaki, P. McMillan, G. C. Sosso, and K. Wynne, "Understanding the emergence of the Boson peak in molecular glasses," *Nat Commun* **14**, 215 (2023).

- ⁶³ C. A. Angell, Y. Yue, L.-M. Wang, J. R. Copley, S. Borick, and S. Mossa, "Potential energy, relaxation, vibrational dynamics and the Boson peak, of hyperquenched glasses," *Journal of Physics: Condensed Matter* **15**, S1051 (2003).
- ⁶⁴ F. Caporaletti, S. Capaccioli, S. Valenti, M. Mikolasek, A. I. Chumakov, and G. Monaco, "Experimental evidence of mosaic structure in strongly supercooled molecular liquids," *Nat Commun* **12**, 1867 (2021).
- ⁶⁵ H. Wagner, and R. Richert, "Equilibrium and non-equilibrium type β-relaxations: D-sorbitol versus o-terphenyl," *The Journal of Physical Chemistry B* **103**, 4071-4077 (1999).
- ⁶⁶ L. Hong, B. Begen, A. Kisliuk, C. Alba-Simionesco, V. N. Novikov, and A. P. Sokolov, "Pressure and density dependence of the Boson peak in polymers," *Physical Review B* **78**, 134201 (2008).
- 67 A. W. Lawson, "Correlation of δS* and δV* in simple activated processes in solids," *J. Phys. Chem. Solids* **3**, 250-252 (1957).
- ⁶⁸ R. W. Keyes, "Volumes of activation for diffusion in solids," *The Journal of Chemical Physics* **29**, 467-475 (1958).
- ⁶⁹ J. Rault, "Glass: Kohlrausch exponent, fragility, anharmonicity," *Eur. Phys. J. E* **35**, 1-28 (2012).
- ⁷⁰ A. Yelon, B. Movaghar, and H. M. Branz, "Origin and consequences of the compensation (Meyer-Neldel) law," *Physical Review B* **46**, 12244-12250 (1992).
- ⁷¹ L. Liu, and Q.-X. Guo, "Isokinetic relationship, isoequilibrium relationship, and enthalpy–entropy compensation," *Chemical Reviews* **101**, 673-696 (2001).
- ⁷² G. Kapteijns, D. Richard, E. Bouchbinder, T. B. Schrøder, J. C. Dyre, and E. Lerner, "Does mesoscopic elasticity control viscous slowing down in glassforming liquids?," *The Journal of Chemical Physics* **155**, (2021).
- ⁷³ J. E. Mark, *Physical Properties of Polymers* (Cambridge University Press, Cambridge; New York, 2004), 3rd Edn.,
- ⁷⁴ L. Hong, P. D. Gujrati, V. N. Novikov, and A. P. Sokolov, "Molecular cooperativity in the dynamics of glass-forming systems: A new insight," *The Journal of Chemical Physics* **131**, 194511 (2009).
- ⁷⁵ K. Z. Takahashi, "Mapping positron annihilation lifetime spectroscopy data of a polymer to classical molecular dynamics simulations without shifting the glass transition temperature," *The Journal of Chemical Physics* **159**, 084903 (2023).
- ⁷⁶ K. Niss, and T. Hecksher, "Perspective: Searching for simplicity rather than universality in glass-forming liquids," *The Journal of Chemical Physics* **149**, 230901 (2018).
- ⁷⁷ N. Mauro, M. Blodgett, M. Johnson, A. Vogt, and K. Kelton, "A structural signature of liquid fragility," *Nature Communications* **5**, 1-7 (2014).
- ⁷⁸ L. O. Hedges, R. L. Jack, J. P. Garrahan, and D. Chandler, "Dynamic order-disorder in atomistic models of structural glass formers," *Science* **323**, 1309-1313 (2009).
- ⁷⁹ M. I. Ojovan, and D. V. Louzguine-Luzgin, "Revealing structural changes at glass transition via radial distribution functions," *The Journal of Physical Chemistry B* **124**, 3186-3194 (2020).
- ⁸⁰ H. R. Wendt, and F. F. Abraham, "Empirical criterion for the glass transition region based on Monte Carlo simulations," *Physical Review Letters* **41**, 1244-1246 (1978).
- ⁸¹ X. Tong, G. Wang, Z. H. Stachurski, J. Bednarčík, N. Mattern, Q. J. Zhai, and J. Eckert, "Structural evolution and strength change of a metallic glass at different temperatures," *Scientific Reports* **6**, 30876 (2016).

- ⁸² K. Georgarakis, D. V. Louzguine-Luzgin, J. Antonowicz, G. Vaughan, A. R. Yavari, T. Egami, and A. Inoue, "Variations in atomic structural features of a supercooled Pd–Ni–Cu–P glass forming liquid during in situ vitrification," *Acta Materialia* **59**, 708-716 (2011).
- ⁸³ W. Tu, S. Valenti, K. L. Ngai, S. Capaccioli, Y. D. Liu, and L.-M. Wang, "Direct evidence of relaxation anisotropy resolved by high pressure in a rigid and planar glass former," *The Journal of Physical Chemistry Letters* **8**, 4341-4346 (2017).
- ⁸⁴ D. Mercier, and J.-C. S. Levy, "Construction of amorphous structures," *Physical Review B* **27**, 1292-1302 (1983).
- ⁸⁵ H. Yoon, and G. B. McKenna, "Testing the paradigm of an ideal glass transition: Dynamics of an ultrastable polymeric glass," *Science Advances* **4**, eaau5423 (2018).
- ⁸⁶ E. Hempel, G. Hempel, A. Hensel, C. Schick, and E. Donth, "Characteristic length of dynamic glass transition near Tg for a wide assortment of glass-forming substances," *Journal of Physical Chemistry B* **104**, 2460-2466 (2000).
- ⁸⁷ M. L. Williams, R. F. Landel, and J. D. Ferry, "The temperature dependence of relaxation mechanisms in amorphous polymers and other glass-forming liquids," *Journal of the American Chemical society* **77**, 3701-3707 (1955).
- ⁸⁸ W. Kauzmann, "The nature of the glassy state and the behavior of liquids at low temperatures," *Chemical Reviews* **43**, 219-256 (1948).
- ⁸⁹ K. Ngai, L., "Structural relaxation and conductivity relaxation in glassy ionics," *J. Phys. IV* **02**, C2-61-C62-73 (1992).
- ⁹⁰ F. Lundin, A. Idström, P. Falus, L. Evenäs, S. Xiong, and A. Matic, "Ion dynamics and nanostructures of diluted ionic liquid electrolytes," *The Journal of Physical Chemistry C* **126**, 16262-16271 (2022).
- ⁹¹ K. I. S. Mongcopa, M. Tyagi, J. P. Mailoa, G. Samsonidze, B. Kozinsky, S. A. Mullin, D. A. Gribble, H. Watanabe, and N. P. Balsara, "Relationship between segmental dynamics measured by quasi-elastic neutron scattering and conductivity in polymer electrolytes," *ACS Macro Letters* **7**, 504-508 (2018).
- ⁹² Y. Doi, J. Allgaier, R. Zorn, S. Förster, T. Egami, and M. Ohl, "Relaxation dynamics and ion conduction of poly(ethylene carbonate/ethylene oxide) copolymer-based electrolytes," *The Journal of Physical Chemistry C* **126**, 20284-20292 (2022).
- ⁹³ M. Lee, H. W. Gibson, T. Kim, R. H. Colby, and U. H. Choi, "Ion–dipole-interaction-driven complexation of polyethers with polyviologen-based single-ion conductors," *Macromolecules* **52**, 4240-4250 (2019).
- ⁹⁴ C. Gainaru, R. Kumar, I. Popov, M. A. Rahman, M. Lehmann, E. Stacy, V. Bocharova, B. G. Sumpter, T. Saito, K. S. Schweizer, and A. P. Sokolov, "Mechanisms controlling the energy barrier for ion hopping in polymer electrolytes," *Macromolecules* **56**, 6051-6059 (2023).
- ⁹⁵ R. Levit, J. C. Martinez-Garcia, D. A. Ochoa, and J. E. García, "The generalized Vogel-Fulcher-Tamman equation for describing the dynamics of relaxor ferroelectrics," *Scientific Reports* **9**, 12390 (2019).
- 96 K. Ngai, and G. Fytas, "Why the relaxation times of polymers from Brillouin light spectroscopy are much shorter than the primary $\alpha\text{-relaxation}$ times," *Macromolecules* **52**, 8305-8311 (2019).